THE JOURNAL OF PHYSICAL CHEMISTRY A
A JOURNAL OF THE AMERICAN CHEMICAL SOCIETY

pubs.acs.org/JPCA Article

Chemistry of Simple Organic Peroxy Radicals under Atmospheric through Combustion Conditions: Role of Temperature, Pressure, and NO_x Level

Mark Jacob Goldman, William H. Green, and Jesse H. Kroll*

Cite This: *J. Phys. Chem. A* 2021, 125, 10303−10314 Read Online

ACCESS | Metrics & More | Article Recommendations | Supporting Information

ABSTRACT: Organic peroxy radicals (RO_2) are key intermediates in the oxidation of organic compounds in both combustion systems and the atmosphere. While many studies have focused on reactions of RO_2 in specific applications, spanning a relatively limited range of reaction conditions, the generalized behavior of RO_2 radicals across the full range of reaction conditions (temperatures, pressures, and NO levels) has, to our knowledge, never been explored. In this work, two simple model systems, *n*-propyl peroxy radical and γ-isobutanol peroxy radical, are used to evaluate RO_2 fate using pressure-dependent kinetics. The fate of these radicals was modeled based on literature data over 250−1250 K, 0.01−100 bar, and 1 ppt to 100 ppm of NO, which spans the typical range of atmospheric and combustion conditions. Covering this entire range provides a broad overview of the reactivity of these species under both atmospheric and combustion conditions, as well as under conditions intermediate to the two. A particular focus is on the importance of reactions that were traditionally considered to occur in only one of the two sets of conditions: RO_2 unimolecular isomerization reactions (long known to occur in combustion systems but only recently appreciated in atmospheric systems) and RO_2 bimolecular reactions of RO_2 with NO (thought to occur mainly in atmospheric systems and rarely considered in combustion chemistry).

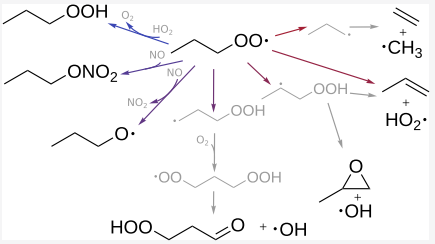

1. INTRODUCTION

Oxidation of organic molecules drives metabolism, precipitates food spoilage,[1] provides for most of the world's electricity and transportation,[2] and controls the formation and degradation of atmospheric pollutants.[3] Since the most abundant atmospheric oxidant, molecular oxygen, is a biradical, oxidation occurs mostly through radical intermediates. An important and ubiquitous class of organic radical intermediates is the organic peroxy radical (RO_2), formed when a carbon-centered radical (R) combines with molecular oxygen. Due to their relative stability, RO_2 radicals can accumulate to high concentrations in oxidation systems and react via a number of competing degradation pathways. Macroscopic phenomena like engine performance,[4] flame propagation,[5] food stability,[1] and atmospheric visibility,[3] all depend on which of the many competing reactions dominates the fate of these transient intermediates.

Figure 1 shows the major pathways by which RO_2 radicals may react, including unimolecular transformations (gray arrows) and bimolecular reactions (red arrows). Bimolecular reaction partners include nitrogen oxides, other peroxy radicals, hydroxyl radicals, and, when concentrations are high, organic molecules. Reaction with NO will form either an alkoxy radical (RO) or an organic nitrate ($RONO_2$).[6] Reaction with other RO_2 radicals forms either two alkoxy radicals, an alcohol and carbonyl (labeled as alkoxy formation and RO_2 recombination in Figure 1, respectively), or a stabilized alkyl peroxide (ROOR).[7,8] RO_2 can also react with NO_2, forming peroxynitrates ($ROONO_2$), but such species are typically thermally unstable except at very low temperatures or when the RO_2 is an acylperoxy radical.[6] RO_2 radicals abstract hydrogen atoms from HO_2 (and at high temperatures, from organic molecules) to form alkyl hydroperoxides (ROOH).[9,10] For particularly stable RO_2 in clean environments, a reaction with OH radicals may also occur.[11] Due to the vast diversity of organic molecules, Figure 1 does not show all pathways, and many other reactions exist for compounds with specific functional groups, such as when alkenes react with RO_2.[12]

In addition to these bimolecular pathways, RO_2 radicals can undergo unimolecular reactions (gray arrows in Figure 1). Intramolecular hydrogen abstraction by the peroxy radical center forms a key oxidation intermediate, the hydroperoxyalkyl radical (QOOH).[13] Other unimolecular pathways include decomposition back to R + O_2[14] and the elimination of HO_2 to form an alkene.[15] If the peroxy radical also has an alkene group, cyclic peroxy alkyl radicals can be formed.[16−19]

QOOH compounds can also undergo a number of subsequent unimolecular reactions. Since QOOH formation

Received: August 13, 2021
Revised: November 5, 2021
Published: November 29, 2021

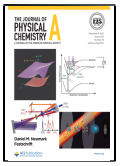

https://doi.org/10.1021/acs.jpca.1c07203
J. Phys. Chem. A 2021, 125, 10303−10314

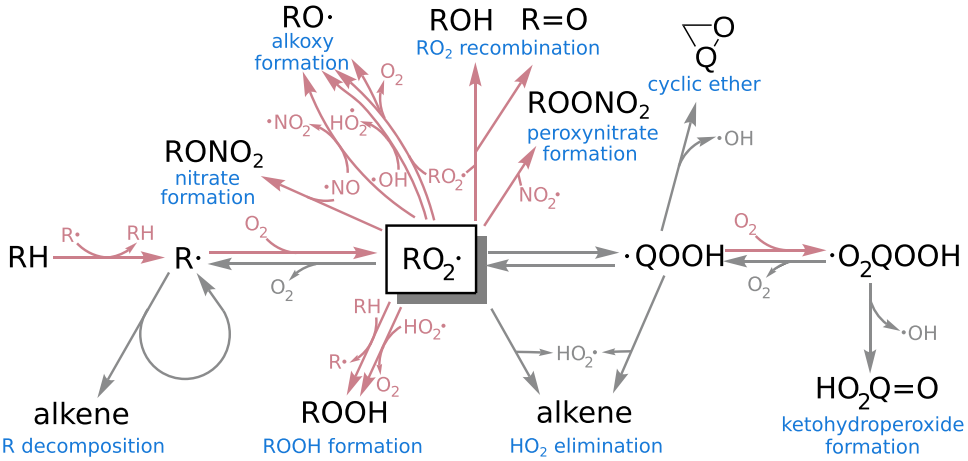

Figure 1. Common unimolecular (gray) and bimolecular (red) reactions of RO_2.

from RO_2 isomerization is often endothermic,[20] QOOH can isomerize back to RO_2. Other competing unimolecular pathways include the formation of a cyclic ether and OH[21] or, in the case where the radical center is adjacent to the hydroperoxide group, an alkene and HO_2.[22] Other pathways, which can occur for specific QOOH structures, are not shown in Figure 1, including the formation of a carbonyl and HO_2,[23] an alkoxy radical and H_2O,[24] and two carbonyl fragments and an OH.[25]

The bimolecular reaction of QOOH with O_2 forms a new peroxy species, the O_2QOOH radical. This can undergo a second intramolecular abstraction of the hydrogen in the hydroperoxide group, which allows for rapid interconversion, or it can abstract the hydrogen on the α-carbon at the base of the hydroperoxide group.[26] If the latter occurs, the hydroperoxide group will often split to form an OH radical and a molecule with both a carbonyl and a hydroperoxide functional group, called a ketohydroperoxide (KHP).[27] The KHP can decompose thermally[27] or photolytically,[28] producing additional OH radicals in the process. Because KHP degradation produces multiple reactive radicals, leading to chain branching, the formation and degradation of KHP play an important role in oxidative environments; this is discussed in detail in the Results section. Its formation has domain-specific names like autoxidation in atmospheric chemistry[29] (which has taken on a somewhat different meaning than in the liquid-phase oxidation literature[7]) and the KHP pathway in the combustion literature.[30] In this work, we refer to the formation of QOOH followed by O_2 addition simply as "isomerization".

Traditionally, RO_2 in the atmosphere has been assumed to react primarily via bimolecular pathways (i.e., with NO_x, HO_2, or RO_2), with unimolecular reactions assumed to be too slow at ambient temperatures to compete. This assumption was based on extrapolating early calculations of the isomerization rates of simple alkylperoxy radicals[31] to more complex alkylperoxy radicals. In contrast, RO_2 chemistry in combustion is usually assumed to be dominated by unimolecular chemistry. However, recent work has shown that this clear bifurcation by regime does not always provide an accurate description of RO_2 chemistry.[15,32−40] Several RO_2 pathways can occur in multiple regimes and are also dependent on the structure of the radicals, suggesting that the RO_2 chemistry known to occur in one regime cannot be discounted in the other.[15,32,34] Here, we discuss two such "crossover" cases: RO_2 isomerization in the atmosphere and bimolecular reactions with NO in combustion systems.

An atmospheric isomerization pathway for isoprene-derived RO_2 radicals was first postulated in 2009 and 2010 to explain an unknown source of OH in forested regions.[41,42] Such pathways were verified experimentally[33] and shown to occur for a wider range of atmospheric RO_2 reactions.[29] Further work showed that alkanes, oxygenates, and alkenes can undergo this pathway in the atmosphere to create highly oxidized molecules that can condense into atmospheric particles,[43−45] which can influence both cloud formation and human health.

Similarly, in combustion systems, the role of RO_2 + NO has been included in only a small fraction of models,[34−37] despite its potential to impact ignition. In particular, the adoption of exhaust gas recycling (EGR), an engine technology that mixes combustion products back into the cylinder inlet to decrease NO_x emissions, has the potential to impact RO_2 chemistry through high concentrations of preignition NO.[37]

Both the combustion chemistry community and the atmospheric chemistry community have benefited, and we conjecture will continue to benefit, from exchanging knowledge of RO_2 chemistry. Though most work is still domain-specific, recent papers have started to bridge the gap by describing the impact of a specific RO_2 pathway in different applications.[15,46−49] In particular, a recent study[49] has experimentally examined RO_2 chemistry over temperatures ranging from 300 to 545 K (atmospheric temperatures up to low-temperature combustion). Other work has evaluated how additional functional groups impact RO_2 fate in specific applications.[20,22,50−53] Here, we take an even more general approach, examining RO_2 branching among a large number of channels (eight in total) and across a wider range of reaction conditions than has been studied previously.

In this study, we investigate the effects of three key parameters on RO_2 reactivity: temperature (which largely affects rates of unimolecular reactions due to their high barrier heights), pressure (which controls collision rates), and NO mixing ratio (which affects bimolecular lifetimes). While the full exploration of the role of RO_2 structure is beyond the scope of this work (due to the very large chemical space involved), we also explore how the addition of a single functional group affects RO_2 chemistry as a function of these conditions. We start with a simple alkylperoxy radical, *n*-propyl peroxy radical (*n*PPR), and then move to a functionalized one, γ-isobutanol peroxy radical (γBPR). These two peroxy radicals were chosen as model systems based on their relatively simple structures (3−4 carbon atoms, 0−1 functional groups) and the fact that their pressure-

https://doi.org/10.1021/acs.jpca.1c07203
J. Phys. Chem. A 2021, 125, 10303−10314

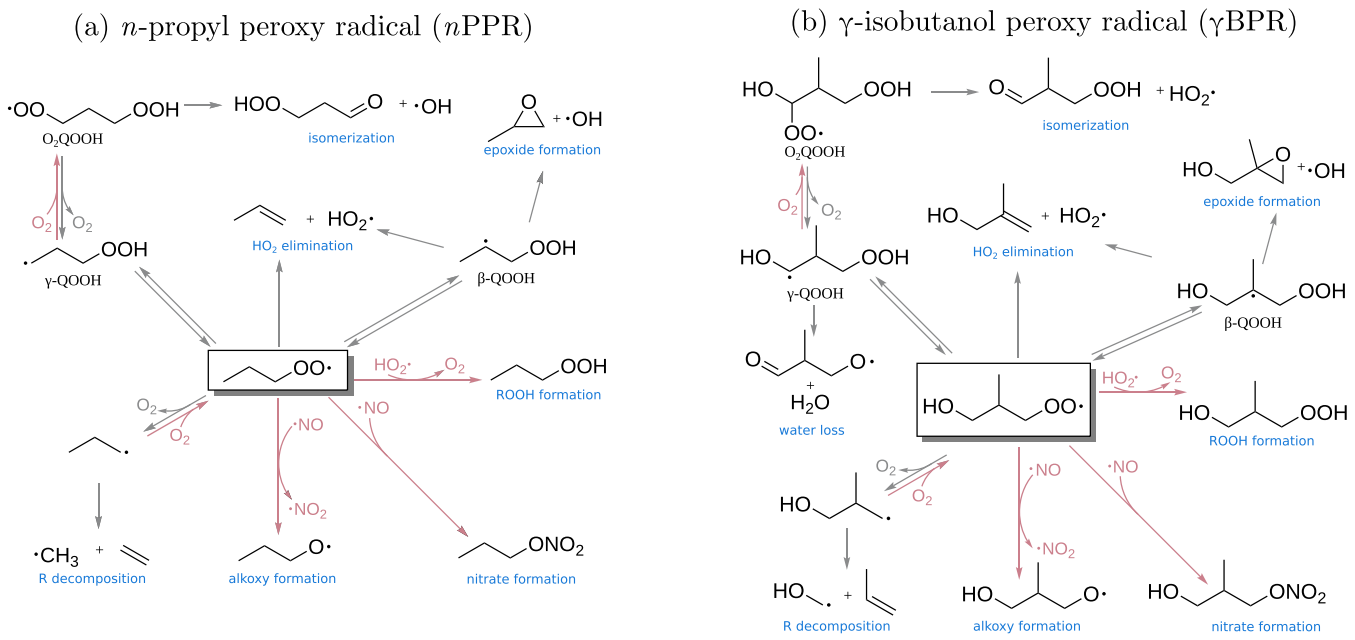

Figure 2. Competing pathways considered in this work, showing unimolecular (gray) and bimolecular (red) reactions. Pathways are labeled with blue text and intermediates are labeled with black text.

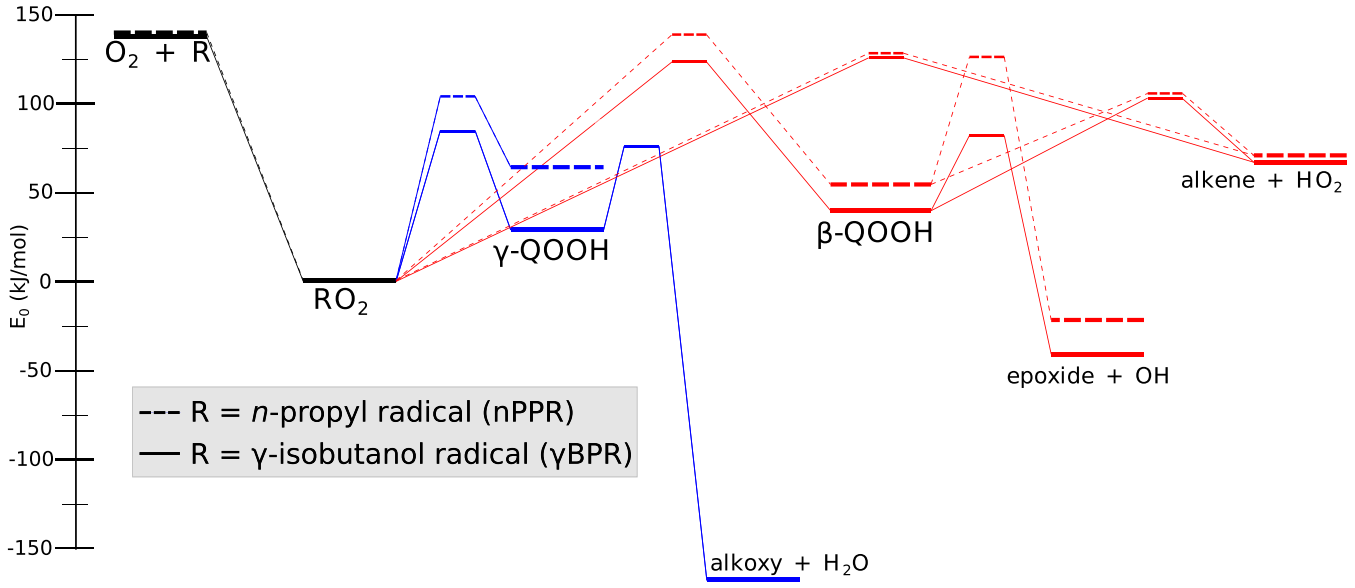

Figure 3. Comparison of potential energy surfaces of *n*PPR[54] (dotted lines) and γBPR[27] (solid lines). Blue-colored pathways involve the γ-QOOH radical and red-colored pathways involve the β-QOOH radical.

dependent kinetics have already been explored in detail.[27,54] By considering the full chemistry of these RO_2 radicals across a wide range of conditions (temperature, pressure, and NO mixing ratio), we are able to explore how these parameters control RO_2 branching, and hence how they control the formation of various products and the extent of radical cycling.

2. METHODOLOGY

Figure 2 shows the peroxy reactions for *n*PPR and γBPR evaluated in this paper. To examine the behavior of RO_2 over a wide range of conditions, we combined kinetic data from a range of sources. The unimolecular reactions for *n*PPR and γBPR originate from recently published pressure-dependent reaction networks based on quantum chemical calculations[27,54] and are compared in Figure 3. Additional details of the kinetic models and simulation scripts are also available in the Supporting Information (SI).

We note that modeling reactivity over such a wide range of reaction conditions necessitates using kinetic parameters that have not been fully validated at all conditions, leading to uncertainties in the simulated kinetics. This work also uses rates from a variety of sources and methods (experiments, quantum calculations, and estimates), which does introduce potential for model error; however, such a combined approach is often employed in detailed kinetic mechanisms.[55,56] We do not expect nor aim for a complete quantitative agreement. Rather, the objective of these simulations is to elucidate the overall dependence of RO_2 reactivity on reaction conditions and

https://doi.org/10.1021/acs.jpca.1c07203
J. Phys. Chem. A 2021, 125, 10303−10314

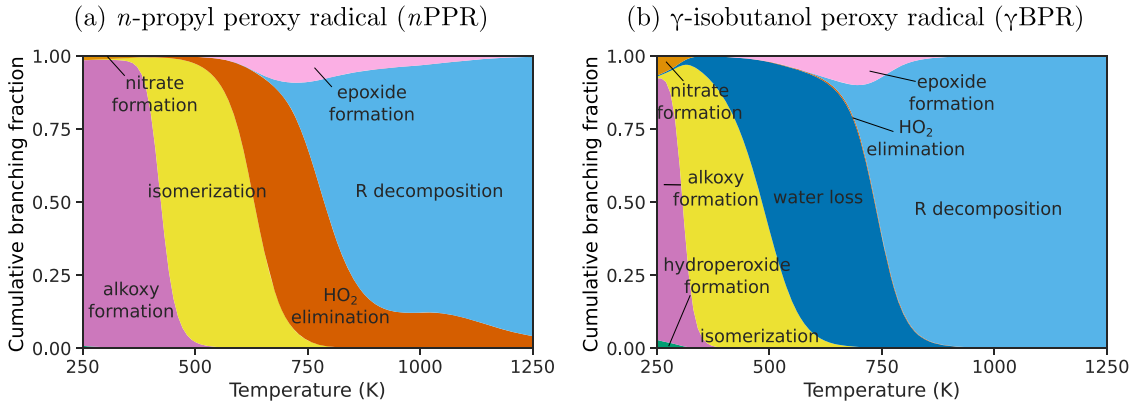

Figure 4. Branching fraction at 0.5 bar and 1 ppb NO over the range of temperatures relevant to atmospheric and combustion conditions. Labels correspond to pathways in Figure 2.

structure; these broad trends are unlikely to be dramatically affected by such uncertainties.

2.1. *n*-Propyl Peroxy Model. All of the reactions in Figure 2a originate from a low-temperature propane combustion model,[30] with the exception of the reactions with NO. This previously published mechanism includes oxidation pathways connecting all of its species to the final oxidation products CO_2 and H_2O. For RO_2 created from the first and second oxygen additions, pressure-dependent rates are obtained from Goldsmith et al., which uses a master equation that was solved using the chemically significant eigenvalue method with quantum calculations at the QCISD(T) level of theory with basis set extrapolation.[27] This combustion model has been validated with experiments at 800−1000 K and 30 bar.[30,57]

The chemistry of NO, NO_2, and HONO is included by adding a combustion NO submechanism that has been validated with experiments from 550 to 1100 K, 1−60 atm, and 0−500 ppm NO.[36] Some additional low-temperature pathways, which were not available in this submechanism, were taken from Atkinson[58] and Jenkin et al.[53] for hydrogen abstraction from an alkoxy radical by O_2 and nitrate formation, respectively.

2.2. γ-Isobutanol Peroxy Model. The γBPR, with one hydroxyl group, is treated as a model system for investigating the impact of functional groups on RO_2 chemistry. This particular species was chosen because of the availability of an extensive pressure-dependent network for its peroxy radical.[54] The pressure-dependent rates originate from solving a master equation with the modified strong collision approximation in the Arkane software package;[59,60] quantum chemical calculations are done using CCSD(T)-F12a/VTZ-F12//B3LYP/CBSB7.

To make the γBPR model complete, bimolecular reactions and subsequent chemistry of their products are added. Kinetics of peroxy reactions with NO and HO_2 are from Jenkin et al.,[53] and hydrogen abstractions by O_2 from alkoxy radicals are from Atkinson.[58] The oxygen addition to the QOOH radical uses kinetics from Miyoshi at the high-pressure limit.[61] Theoretical calculations and experimental data indicate that the oxygen addition to γ-QOOH followed by HO_2 elimination is likely to be faster than the direct hydrogen abstraction reaction to form HO_2;[62] therefore, the latter pathway was not included in this study. The isomerization of O_2QOOH to form a ketohydroperoxide with an additional hydroxy group (not shown in Figure 2) is from analogous reactions reported in a study by Yao et al.,[20] and the isomerization to form the ketohydroperoxide is from the analogous reaction reported in a study by Goldman et al.,[54] both at the high-pressure-limit. (This contrasts with the treatment of unimolecular reactions of γBPR, which uses pressure-dependent kinetics). The kinetics for the decomposition of the γ-isobutanol radical, termed "R decomposition", is from a study by Sarathy et al.[63]

2.3. Other Compounds. In addition to *n*PPR and γBPR, this paper also uses model RO_2 radicals originating from other molecules to give a broader perspective of how structure impacts peroxy fate. For these systems, RO_2 branching was either obtained based on modifications to isomerization rates at atmospheric conditions (butane, isopentane, and 2-butanol)[50] or from published mechanisms without pressure-dependent kinetics.[56] Details are given in Section S1 of the SI. While such results are not as accurate as those from the full network, they still enable insights into how RO_2 structure controls branching and radical cycling, as discussed at the end of Section 3.

2.4. Simulations. All simulations were conducted using the kinetic solver Cantera package.[64] Starting mixtures were simulated at constant pressure and temperature unless otherwise noted. Simulations involve starting with the parent alkyl radical (R), following the subsequent chemistry, and determining the pathway from the product distribution. An initial alkyl radical mole fraction (mixing ratio) of 10^{-17} was used to minimize the effect of organic+organic (e.g., $RO_2 + RO_2$) reactions since RO_2 concentrations can vary significantly across the range of temperatures evaluated. A consequence of this low concentration is that $RO_2 + RO_2$ reactions are not examined in this work. Such reactions can be important under some conditions, but they introduce substantial complexity to the reaction system, as product formation becomes highly dependent on starting conditions. For this reason, the bimolecular reactions of RO_2 other than with HO_2 and NO are beyond the scope of this study; such reactions (and the consequent dependencies on starting concentrations) are important topics for future work in this area. Unless otherwise noted, the mole fraction of HO_2 was set as 10^{-11} to approximate atmospheric mixing ratios (note that this is lower than the HO_2 concentration in typical combustion systems). The remaining gas is a mixture of oxygen and nitrogen in a 21:79 ratio.

The simulation is run until the concentration of the alkyl radical, and its corresponding peroxy radical are <1% of the initial alkyl radical concentration. The final product concentrations are mapped to their formation pathway to determine the branching ratio of RO_2. Which products correspond to which pathways are described in Table S1 of the SI. Some reactions in

https://doi.org/10.1021/acs.jpca.1c07203
J. Phys. Chem. A 2021, 125, 10303−10314

the *n*PPR network were removed to allow proper tracing of radicals; these are listed in Table S3 of the SI.

Starting the simulation with the alkyl radical and presenting the final product composition allows this work to account for pressure-dependent effects (in which an excited RO_2 can react to form QOOH, R + O_2, or other products before losing energy through deactivating collisions). This gives a more complete picture of the products than would be obtained from looking at the reaction rates from a thermally equilibrated RO_2, which gives only instantaneous branching ratios.

This work also seeks to understand how these pathways influence the formation of OH and HO_2. To do this, characteristic decomposition pathways are outlined for each pathway (shown in Figures S2−S12 of the SI), and the number of radicals produced in each pathway is shown in Table S5 of the SI. Radical production is determined by multiplying the fraction of RO_2 proceeding via each pathway by the radical yield from that pathway.

3. RESULTS

3.1. Temperature Dependence. Figure 4a shows the product distribution of *n*PPR across a range of temperatures, from low temperatures found near Earth's surface (250−325 K) to relatively high combustion temperatures where RO_2 radicals no longer play an important role. The simulations included 1 ppb of NO at 0.5 bar. (The role of NO and pressure will be examined in later sections.) At the lower end, *n*PPR reacts bimolecularly with abundant NO forming mostly alkoxy radicals and some alkyl nitrates.

At higher temperatures, unimolecular transformations start to dominate. The dominant pathway at 600 K is the isomerization pathway shown in Figure 2a, which involves two H-migration reactions followed by decomposition to form a KHP and an OH radical. The KHP can further break down and release two additional OH radicals.[30] At higher temperatures, around 750 K, *n*PPR predominately decomposes to propene and HO_2. This HO_2 elimination occurs either directly from RO_2 or through a β-QOOH intermediate (which is also the intermediate that forms an epoxide).

The transition between isomerization and HO_2 elimination channels is a competition between two unimolecular reactions: a six-membered cyclic transition state that forms a γ-QOOH (which is more competitive at lower temperatures) and a five-membered transition state that can either lead directly to HO_2 and alkene or form a β-QOOH. With higher temperatures, the impact of the activation energy decreases, making entropic differences more important. Since the five-membered ring involves a smaller entropy penalty and a higher activation energy, it more readily competes at higher temperatures. Determination of how much HO_2 and alkene are formed directly from RO_2, as opposed to indirectly through a β-QOOH intermediate, is made difficult because the pressure-dependent reaction of excited β-QOOH* ($RO_2 \rightarrow \beta$-QOOH* $\rightarrow HO_2$ + alkene) appears in the kinetic mechanism as direct formation from RO_2. The reactions are also complicated by the reverse reaction, QOOH $\rightarrow RO_2$, which can also occur in an excited state. The competition between these pathways is discussed in depth in a study by Merchant et al.[30]

The transition from isomerization to HO_2 elimination leads to an overall decrease in reactivity with increasing temperature because the latter does not produce the more reactive OH radical. This particular transition is important in combustion since it means that an increase in the initial temperature of combustion increases the time necessary for autoignition. This temperature range, known as the negative temperature coefficient regime, results from the fact that the products of HO_2 elimination (HO_2 + alkene) are significantly less reactive than the OH radicals formed from the isomerization pathway.[65] Such an effect is slightly dampened by the epoxide formation, which also releases OH and occurs in the same temperature range as HO_2 elimination, but its effect is secondary because it is not a dominant pathway and the breakdown of the epoxide does not release as many OH as the decomposition of the KHP.

At the highest temperatures (>1000 K), the *n*-propyl decomposes into ethene and methyl radical before even reacting with O_2 to form RO_2; thus, RO_2 chemistry does not play a role in oxidation at such high temperatures. The extension of the HO_2 elimination and epoxide formation in Figure 4a above 1000 K is an artifact of how the rate constants were fit (see Section S4 of the SI for more information).

3.2. Effect of the −OH Group. Figure 4b shows branching ratios as a function of temperature for the γBPR, revealing the effect of the OH moiety on the product branching of RO_2. This radical's reactivity has the same overall features as the unsubstituted peroxy radical (Figure 4a), namely, the dominance of bimolecular reactions at low temperatures, unimolecular reactions at higher temperatures, and decomposition at the highest temperatures.

However, the presence of the OH group leads to a number of key differences as well. First, the OH group weakens the nearest C−H bond, which is reflected in the lower barrier height of γBPR in forming γ-QOOH in Figure 3. This decreases the activation energy needed to isomerize, allowing for the isomerization involving a six-membered transition state to occur at lower temperatures, and increases the stability of QOOH, reducing the reverse reaction rate.[29] After forming γ-QOOH, isomerization proceeds differently in *n*PPR and γBPR. For γBPR, O_2 abstracts the H from the hydroxy group (top left of Figure 2b), forming the KHP plus an HO_2 instead of an OH. This pathway is significantly faster than the standard isomerization channel, which forms an OH instead (Figure 2a). Both pathways form a KHP, which can produce two additional OH radicals upon further degradation.

The presence of the OH functional group also introduces additional reaction pathways. The intramolecular hydrogen abstraction to form QOOH can be followed by another hydrogen abstraction in which the radical oxygen on the hydroperoxy group abstracts the hydrogen on the alcohol while simultaneously breaking the O−O bond, forming water and a ketoalkoxy radical (water-loss pathway in Figure 2b).[24] This reaction has a lower barrier than any other unimolecular pathway in Figure 3, allowing it to compete at lower temperatures with the O_2 addition necessary for isomerization. Previous work showed that inclusion of this pathway was necessary to describe the high yield of acetaldehyde in isobutanol oxidation.[24,66]

This additional fast water formation pathway also pushes up the temperature at which HO_2 elimination can become competitive. Since HO_2 elimination has a smaller five-membered cyclic transition state, its entropy of activation is lower, and so it becomes more dominant at higher temperatures; however, R decomposition takes over before HO_2 elimination becomes competitive with water formation. Thus, HO_2 elimination is never the dominant channel for γBPR.

As shown in Figure 3, the barrier to epoxide formation on the γBPR surface is substantially lower than that of *n*PPR. This can

https://doi.org/10.1021/acs.jpca.1c07203
J. Phys. Chem. A 2021, 125, 10303−10314

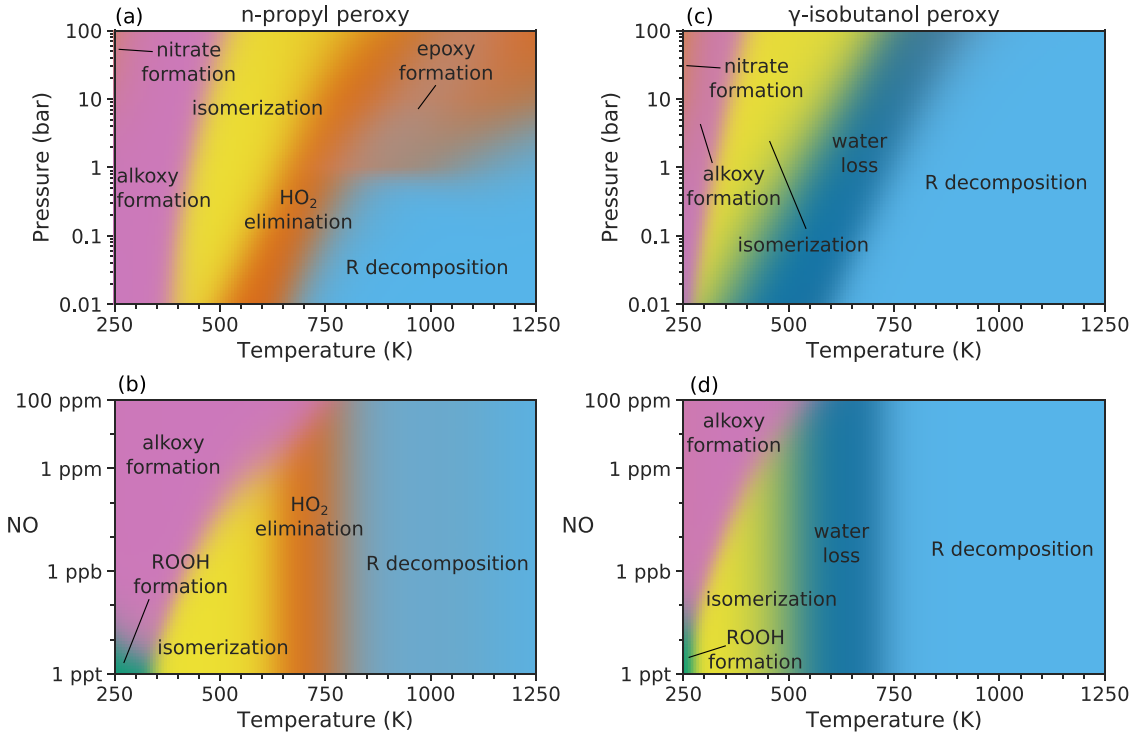

Figure 5. Major products from R + O_2 after 99% conversion. Panels (a) and (c) show the branching ratios of *n*PPR and γBPR at various temperatures and pressures, with the NO mixing ratio fixed at 1 ppb. Panels (b) and (d) show the branching ratios of *n*PPR and γBPR at various temperatures and NO mixing ratios at 0.5 bar pressure. Names correspond to reactions in Figure 2. Colors are linear combinations of those used in Figure 4 to designate individual pathways. The abrupt transition in panel (a) between 800 and 1000 K is an artifact of fitting pressure-dependent parameters and is discussed in Section S4 of the SI.

be partially attributed to the presence of a hydrogen bond from the hydroxyl group stabilizing the transition state's epoxide-forming oxygen. The additional alkyl groups, such as the CH_3 group in β-QOOH, may also aid in decreasing the ring strain relative to the open structure. With this lower barrier, epoxide formation in γBPR more effectively competes with water formation than HO_2 elimination.

In summary, the addition of functional groups can lead to dramatic changes in RO_2 reactivity and radical cycling. This arises from different effects: changes in bond strengths, formation of hydrogen bonds, and introduction of new reaction pathways. The addition of other functional groups (such as peroxides, carbonyls, alkenes, etc.) will likely have similar effects on RO_2 reactivity, as they also weaken C−H bonds and thus will promote isomerization;[50] they may also introduce new unique reaction channels.[67]

3.3. Pressure Dependence. While Figure 4 shows that temperature variation strongly impacts product formation, it masks the interplay between the temperature and other key physical parameters, such as pressure and bimolecular reactant concentrations.

Figure 5 highlights the impact of two key reaction parameters (pressure and NO level) on branching ratios. Colors denote the expected product mixture at a given set of conditions; the color at any location in Figure 5 results from a linear combination of colors representing a single RO_2 reaction channel (used in Figure 4) weighted by the branching ratio of each. As in Figure 4, under most conditions, a single pathway dominates. Across the full range of pressures, the mixing ratio is held constant. Because of this, the concentrations of bimolecular reactants, namely HO_2, NO, and O_2, increase proportionally with pressure. Figure 5a,c focus on the temperature and pressure dependence of *n*PPR and γBPR, respectively.

For an adiabatic system, a change in pressure has a smaller effect on branching ratios than the corresponding change in temperature. At any given pressure, across the factor-of-five temperature range (250−1250 K), the system passes through four sets of dominant reaction products. But fewer shifts in the chemical regime are seen when the temperature is held constant and pressure is changed by a much larger amount (four orders of magnitude). Using the example of *n*PPR at 300 K with a fixed NO mixing ratio, the dominant reaction product does not change across the entire 0.01−100 bar pressure range shown in Figure 5a.

The impact of pressure on branching ratios in Figure 5a,c arises from two effects: change in pressure-dependent rate coefficients and change in bimolecular reactant concentration. For both compounds, the latter effect dominates the former. For example, at 1000 K, the rate coefficient for *n*PPR to propene and HO_2 increases by a factor of 250 over the range 0.01−100 bar; this change is small compared to the corresponding 10^4 increase in O_2 concentration, which would dramatically enhance some competing bimolecular reaction rates.

Competition between pathways that differ in the extent of bimolecular reactions is dominated by this concentration effect. This happens to be the case for three transitions in Figure 5a,c, corresponding to the three branching points in Figure 1 that involve unimolecular and bimolecular pathways: bimolecular reactions with RO_2, O_2 addition to QOOH, and O_2 addition to R. In each case, the bimolecular reaction benefits from the higher molecular density at higher pressures, leading to a similar slope at all three transitions for both *n*PPR and γBPR. At lower temperatures, the effect of pressure is largely due to an increase

https://doi.org/10.1021/acs.jpca.1c07203
J. Phys. Chem. A 2021, 125, 10303−10314

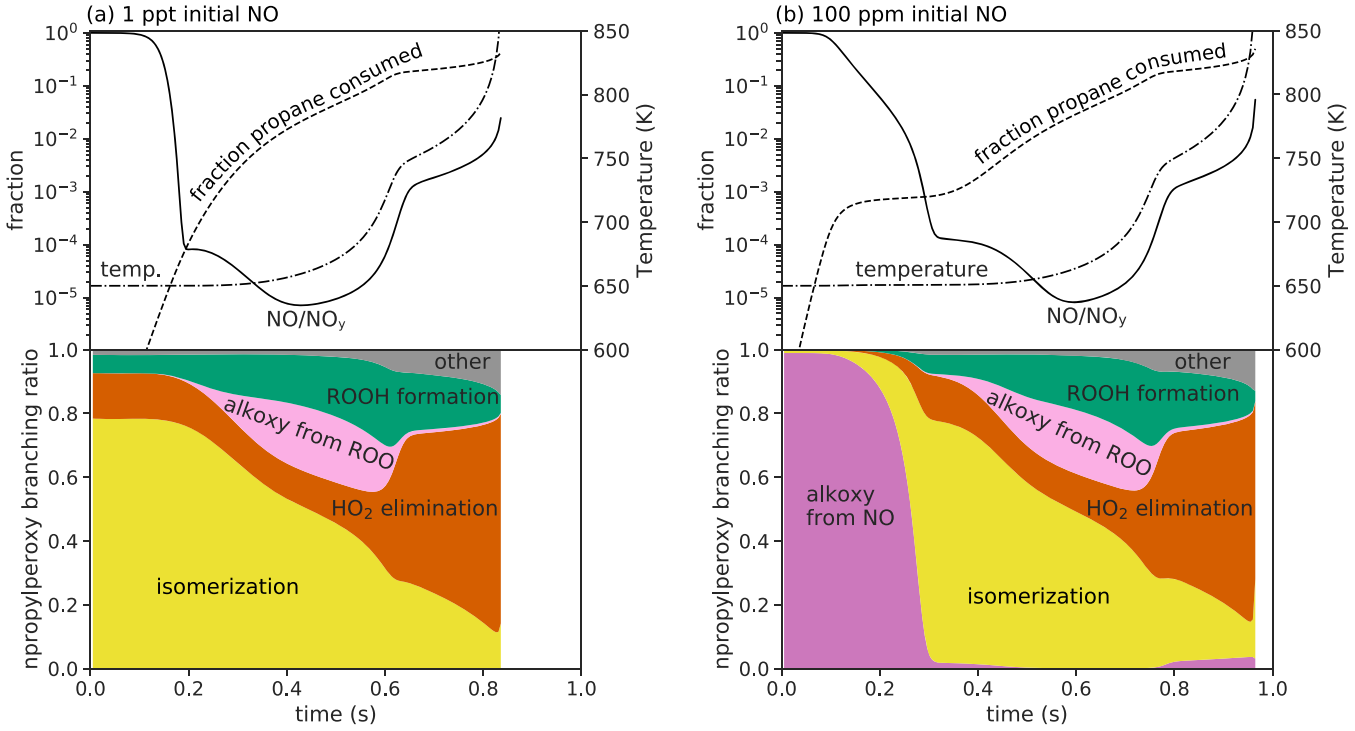

Figure 6. Properties of propane preignition at various initial NO mixing ratios: (a) 1 ppt and (b) 100 ppm. The top panels show the fraction of NO_y (= NO + NO_2 + HONO) as NO (solid lines), the fraction of propane reacted (dashed lines), and the system's temperature (dot-dashed lines). The bottom graphs show instantaneous peroxy branching ratio over the course of the simulation, which was calculated based on the rate of various RO_2-consuming reactions and is listed in Table S2 of the SI. Simulations involved an adiabatic, constant-volume system starting at 650 K and 10 bar in air with a fuel/oxygen equivalence ratio of 1.

in the number density of bimolecular reactants, which defines the boundary between RO_2 bimolecular reactions and isomerization. In the next transition, the unimolecular HO_2 elimination competes with the isomerization sequence leading to KHP since the critical bimolecular QOOH + O_2 step in that sequence depends on O_2 concentration. At the highest temperatures, the bimolecular formation of RO_2 competes with the unimolecular decomposition of the alkyl radical, also leading to a competition that depends on O_2 density.

While the dominant pressure effect in Figure 5a,c comes from concentration, pressure-dependent rate coefficients can still impact critical transition points. This can be assessed by finding the branching fraction when we use the rate coefficients corresponding to the actual pressure of a system and compare that to the branching fraction obtained using rate coefficients near the high-pressure limit. For *n*PPR at 600 K, which is near an important transition in combustion chemistry, isomerization has a branching ratio of 5%. If one were to apply the rate coefficients at 100 bar to this system, which approximates the high-pressure limit, the branching ratio of isomerization would increase to 77%. This is a substantial change, and it indicates that pressure-dependent kinetics are important in this regime, even if they affect the system properties less than concentration and temperature. For more details about the specific pressure-dependent effects for these two systems, see Goldsmith et al. and Goldman et al.[27,54]

3.4. NO Dependence. Reactions of RO_2 with NO, which primarily form alkoxy radicals, can also have a significant effect on oxidative processes. The alkoxy radical has a higher propensity to break C−C bonds and to undergo intramolecular H-abstraction than the analogous peroxy radicals, leading NO to influence the final product distribution. The reaction with NO can also form an organic nitrate that can sequester NO_x (and HO_x) in the atmosphere. Figure 5b,d show the effect of NO and temperature on the branching of *n*PPR and *γ*BPR, respectively.

At low temperatures and low NO mixing ratios, the dominant fate of RO_2 is the reaction with HO_2, forming organic hydroperoxides (ROOH). As NO mole fraction increases, the bimolecular reactant shifts from HO_2 to NO, leading to the formation of an alkoxy radical instead of ROOH. Increasing NO concentration also increases the temperature necessary for isomerization to compete with RO_2 + NO. Figure 5a,c are based on an NO concentration of 1 ppb; a lower NO concentration, which is typical of most of the atmosphere, would result in isomerization occurring at lower temperatures than shown.

For *n*PPR (Figure 5b), when NO is greater than 1 ppm, isomerization ceases to dominate at any temperature, which could impact combustion engines run under initially high NO concentrations.[68,69] The isomerization cutoff for *γ*BPR in Figure 5d requires more NO since its isomerization pathway is faster. Above 800 K for both compounds, unimolecular reactions always dominate, preventing even high concentrations of NO from affecting branching ratios.

3.5. RO_2 + NO Impact on Engine Preignition. In most treatments of low-temperature combustion, preignition (the time before the fuel-air mixture ignites) is influenced by the competition between two unimolecular RO_2 pathways: isomerization and HO_2 elimination pathways.[30] Figure 5 suggests that, with enough NO, bimolecular reactions may overtake these unimolecular pathways, which has the potential to change the product distribution and ignition characteristics of the reaction system.

As shown in Figure 5a,c, at high temperatures and pressures (650 K and 1 bar), reaction with NO cannot compete with

https://doi.org/10.1021/acs.jpca.1c07203
J. Phys. Chem. A 2021, 125, 10303−10314

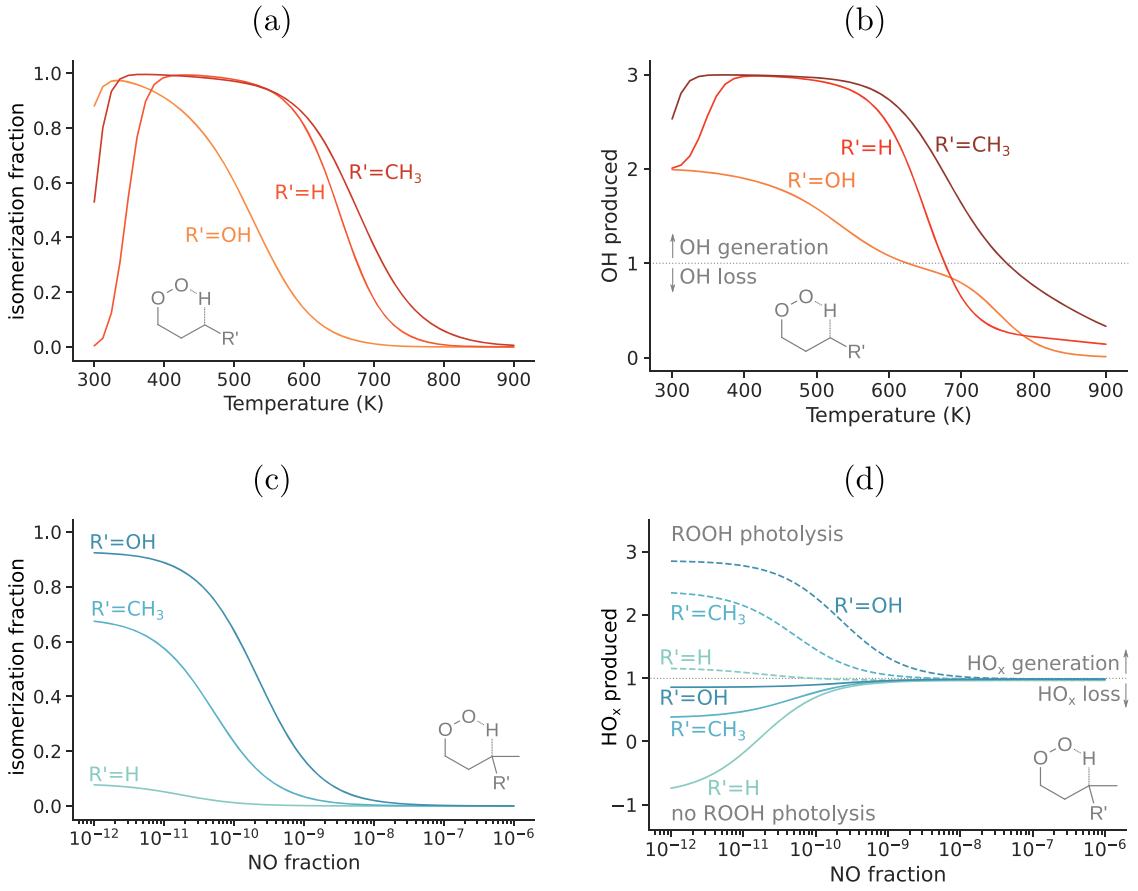

Figure 7. Dependence of RO_2 reaction pathways and radical cycling on key reaction conditions and RO_2 substitution. Panels (a) and (b): the isomerization fraction and number of OH radicals produced from various RO_2 radicals as a function of temperature (no NO, 1 bar pressure). Panels (c) and (d): the isomerization fraction and number of HO_x ($OH + HO_2$) radicals produced from various RO_2 radicals as a function of NO mixing ratio (298 K, 1 bar). Each curve is labeled by the identity of the R' (H, CH_3, OH) group shown on the gray transition state structures; in panels (a) and (b), the "OH" calculation is for isobutanol, which also has a methyl group on the β-carbon.

isomerization at ppb levels of NO. Thus, for NO to affect RO_2 branching ratio in preignition chemistry, there must be an additional source of NO. NO and NO_2 are typically produced during and after ignition through various high-temperature pathways, with the dominant pathway requiring the thermal breakdown of O_2 above 2000 K.[70] EGR engines, which intentionally recycle postcombustion gas back into the engine, can obtain higher preignition NO concentrations in the ppm range, allowing reactions with NO to compete with isomerization.

However, elevated levels of NO will affect ignition only if they remain high during the entire ignition process. If NO is instead converted to other forms of oxidized nitrogen (e.g., NO_2, HONO), the system's position in Figure 5b,d would shift downward, decreasing the impact of RO_2 + NO chemistry on combustion. To investigate this effect, we carry out adiabatic, constant-volume simulations of propane in air, with a molar ratio of propane to O_2 of 1:4.5 (stoichiometric ratio of 1) and either 1 ppt or 100 ppm of initial NO to emulate non-EGR and EGR engines, respectively. Unlike the previous simulations of RO_2 branching, where HO_2 concentrations did not vary (Figures 4 and 5), HO_2 levels are explicitly calculated in this simulation to more accurately capture combustion phenomena.

Simulation results (key concentrations, temperatures, and RO_2 branching ratios) are shown in Figure 6. During preignition under both conditions, the concentration of NO drops rapidly as it gets converted to NO_2, thereby dampening its effect on peroxy radical fate. During this process, NO increases the initial reactivity of the system, which is shown by the steeper propane consumption slope in the 100 ppm NO case. However, once most of the NO is converted into NO_2, the consumption of propane slows significantly. This period of inactivity from 0.15 to 0.4 s is driven by the reaction $HO_2 + NO_2 \rightarrow HONO + O_2$, which consumes radicals and slows ignition. (The termolecular reaction of HO_2 and NO_2 to form HO_2NO_2, which is important in atmospheric HO_x-NO_x chemistry, is not significant at elevated temperatures and so was not included in the mechanism.) After 0.4 s, most NO_2 and NO have been consumed and the RO_2 chemistry of the high-initial-NO case (Figure 6b) resembles that of the low-initial-NO case (Figure 6a), with low-temperature isomerization initially dominating followed by HO_2 elimination. Overall, the ignition timing (defined as the time the system takes to reach a temperature of 1000 K) in the two cases differs by less than 20%; this minor difference is predominantly due to the decrease in reactivity from HONO formation balancing out the highly reactive alkoxy radicals formed from NO + RO_2. Thus, while NO from EGR can increase the system's initial reactivity via the bimolecular reaction of RO_2 + NO, NO is rapidly consumed. The NO_2 then sequesters HO_2 to form HONO, largely canceling out much of the reactivity increase from the RO_2 + NO reaction. The chemistry then reverts to low-NO conditions, with

https://doi.org/10.1021/acs.jpca.1c07203
J. Phys. Chem. A 2021, 125, 10303−10314

subsequent RO_2 chemistry dominated by unimolecular reactions.

3.6. RO_2 Isomerization and Radical Cycling. In addition to representing key branch points in oxidation processes, RO_2 radicals play a key role in radical cycling for both atmospheric and combustion systems. A given RO_2 pathway may lead to chain termination, chain propagation, or chain branching, and this competition can have a major influence on the subsequent reactivity of the system. This interplay between RO_2 chemistry and radical cycling, which is affected by the reaction conditions and the presence of functional groups, is examined in Figure 7.

Figure 7a shows the role of temperature and structure in controlling the fate of RO_2 radicals, specifically the fraction that undergoes isomerization (intramolecular H-atom transfer). Calculations are for 1 bar pressure, no NO, and an HO_2 mixing ratio of 10 ppt. For unsubstituted and OH-substituted radicals, results are the same as in Figure 4; isomerization occurs only at high temperatures for the unsubstituted RO_2 but dominates even at room temperature for the OH-substituted RO_2. The methyl-substituted RO_2 represents the intermediate case, with a barrier and hence an isomerization rate in between the two. At higher temperatures (>400 K), the isomerization fraction drops with temperature due to the increasing importance of competing unimolecular channels. This occurs first for the OH-substituted RO_2 due to the increasing importance of the water-loss channel, and then for the other RO_2 species, which at high temperatures undergo HO_2 elimination.

In low-temperature combustion, the number of OH radicals formed from a single RO_2 radical is a critical driver of the overall reactivity of the system. Figure 7b shows this OH production from RO_2 radicals as a function of temperature, based on the branching ratio to various pathways and their corresponding OH yields (given in Table S5 of the SI). The formation of exactly one OH radical propagates the oxidation chain (shown as a dotted line in Figure 7b); the formation of more than one OH contributes to chain branching, accelerating the oxidation process and thus increasing the temperature of the system, bringing combustion systems closer to ignition (this temperature change is immeasurably small under atmospheric conditions due to low concentrations and slow reaction rates); and the formation of less than one OH contributes to chain termination, slowing down the ignition process. RO_2 isomerization reactions are critical to this branching: the isomerization of an alkylperoxy radical, followed by a second isomerization of the resulting O_2QOOH radical, leads to the formation of an OH (Figures 1 and 2a), and the thermal degradation of the resulting KHP can form two more.[30] However, this OH formation drops rapidly at higher temperatures, as other reaction channels outcompete isomerization, causing a decrease in reactivity in the negative temperature coefficient region. In the case of the OH-substituted RO_2, isomerization initially forms HO_2 rather than OH, so only 2 OH radicals are formed; this lower OH production also drops off rapidly with temperature as the water-loss channel begins to dominate. Thus, even for the very simple RO_2 radicals considered here, radical formation, and hence the timing of ignition in combustion systems, is a strong function of the structure of the RO_2 radical.

The role of functional groups in RO_2 fate is explored for conditions relevant to the atmosphere in Figure 7c,d; these are similar to Figure 7a,b, except that they show the dependence on NO rather than temperature, and focus on overall HO_x (OH + HO_2) production rather than just OH production. Figure 7c shows the fraction of RO_2 undergoing isomerization as a function of NO (300 K, 1 bar, and an HO_2 mixing ratio of 10 ppt). The results for unsubstituted and OH-substituted RO_2 are consistent with Figure 4: at very low NO, the isomerization fraction depends on the isomerization rate (since it competes with RO_2 + HO_2, whose rate is assumed to be fixed) and drops with increasing NO. As in Figure 7a, the CH_3-substituted RO_2 is an intermediate case.

As in combustion systems, RO_2 chemistry is critical to the cycling of radical species in the atmosphere. In particular, it can control the levels of HO_x radicals, which play a central role in tropospheric oxidation rates and ozone production. Figure 7d shows the number of HO_x radicals produced from a given RO_2 molecule as a function of NO level, as determined from RO_2 branching ratios and HO_x yields (see Figures S2−S12).

Two curves are shown for each RO_2 radical; these denote the range of possible HO_x cycling, depending on the assumed fate of the organic reaction products. Solid lines denote the HO_x co-produced with the organic reaction products, which are assumed not to degrade further. At high NO, the RO_2 + NO reaction dominates, usually forming a single HO_x radical, and the system is chain-propagating. (For the small RO_2 species here, organic nitrate formation, which produces no HO_x radicals, is a minor channel.) At the other extreme, at low NO, there is a competition between RO_2 + HO_2 to form ROOH (chain termination) and RO_2 isomerization (chain propagation); this competition, and the ultimate change to HO_x at low NO, depends on the isomerization rate.

Dashed lines in Figure 7d denote HO_x produced if any hydroperoxide products are assumed to decompose (either photolytically or thermally), forming an alkoxy radical and an OH. This typically produces two more HO_x than produced without peroxide decomposition and represents a rough upper limit to HO_x production. In this case, the low-NO chemistry of some RO_2 can serve as a source of HO_x radicals via decomposition of the KHP produced in chain-propagating isomerization reactions. This is similar to radical cycling from RO_2 in low-temperature combustion (Figure 7b), except that it involves photolytic rather than thermal degradation of the peroxide species. Such HO_x production from low-NO RO_2 chemistry has been proposed previously in the case of isoprene oxidation.[41,71] It may occur for RO_2 radicals formed from other volatile organic compounds as well, but this depends critically on the extent to which the peroxide products undergo photolysis. Unfortunately, the atmospheric fate of functionalized organic peroxide species is poorly constrained at present; due to its importance in atmospheric radical cycling, this is an important area for future research.

4. CONCLUSIONS

This study maps out the reactivity of small RO_2 radicals of various structures, covering the full range of temperature, pressure, and NO mixing ratio found across both atmospheric and combustion conditions. For the simple systems examined here, results show a complex interplay between the structure and reaction conditions in determining reaction pathways followed. The temperature has a controlling influence on RO_2 branching, with bimolecular reactions dominating at lower temperatures. At higher temperatures, unimolecular channels become increasingly important: first are isomerization reactions (forming KHP species), then fragmentation reactions (such as HO_2 elimination or water-loss channels), and finally, at temperatures approaching ignition, decomposition back to R + O_2. NO mixing ratios and system pressures also play a major role in determining RO_2

https://doi.org/10.1021/acs.jpca.1c07203
J. Phys. Chem. A 2021, 125, 10303−10314

branching by controlling the rates of bimolecular reactions, but these effects, while often important, are generally not as dramatic as the temperature dependence. RO_2 + NO reactions are unlikely to play a major role in most combustion systems since NO (and NO_2) levels will quickly be depleted in fuel combustion processes.

Moreover, the RO_2 structure plays a dominant role in product branching: the addition of even one functional group can have a dramatic influence on energetics (e.g., weakening adjacent C−H bonds to promote isomerization reactions), as well as introduce new reaction channels. These effects can have a governing influence on the organic product distribution, which controls processes such as organic aerosol formation in the atmosphere, as well as on subsequent radical cycling, which is central to virtually all oxidation systems. The degree of radical cycling (whether the system is chain branching, propagating, or terminating) depends critically on the RO_2 structure, reaction conditions (temperature and NO level), and the fate of the RO_2 reaction products.

While this work covers key aspects of the branching of a few simple RO_2 radicals over a wide range of conditions, additional work is needed to understand the fate of organic peroxy radicals generally. Specific to the models in this work, the fate of radical products, such as those from the alkoxy formation, water formation, and R decomposition pathways, should be evaluated to better understand the impact of each pathway on the system-wide behavior. Furthermore, larger and more structurally complex RO_2 (with rings, branches, and multiple functional groups) will generally exhibit reactivity that is substantially more complex than the simple model systems examined here. Improved descriptions of the chemistry of bimolecular coreactants (e.g., RO_2 + RO_2 reactions, the detailed NO_x mechanism) will also lead to more complete descriptions of RO_2 chemistry under a wide range of conditions. Peroxy radicals in other phases (such as in liquid organic matrices, aqueous solutions, and at interfaces) may also exhibit substantially different reactivities. Experiments will continue to be critical not only for validating pathways but also for finding new pathways. Leveraging experiments and calculations to further validate branching in transition regions will provide a more quantitative understanding of products for use in models, and may lead to a general methodology to evaluate RO_2 fate across domains. This would enable the evaluation of peroxy fate for more complex compounds found in the atmosphere, in fuels, and in other organic oxidation systems.

■ ASSOCIATED CONTENT

Supporting Information

The Supporting Information is available free of charge at https://pubs.acs.org/doi/10.1021/acs.jpca.1c07203.

Information on the matching of products to reaction pathway; information on which reactions were removed to allow matching of products with specific paths for the *n*PPR system; a plot showing the unsmooth behavior when changing pressure for the *n*PPR system; and a detailed description of the chemistry (including OH and HO_2 yields) used to derive Figure 7 (PDF)

■ AUTHOR INFORMATION

Corresponding Author

Jesse H. Kroll − *Department of Civil and Environmental Engineering, Massachusetts Institute of Technology, Cambridge, Massachusetts 02139, United States; Department of Chemical Engineering, Massachusetts Institute of Technology, Cambridge, Massachusetts 02139, United States;* orcid.org/0000-0002-6275-521X; Email: jhkroll@mit.edu

Authors

Mark Jacob Goldman − *Department of Chemical Engineering, Massachusetts Institute of Technology, Cambridge, Massachusetts 02139, United States;* orcid.org/0000-0001-8908-3356

William H. Green − *Department of Chemical Engineering, Massachusetts Institute of Technology, Cambridge, Massachusetts 02139, United States;* orcid.org/0000-0003-2603-9694

Complete contact information is available at: https://pubs.acs.org/10.1021/acs.jpca.1c07203

Notes

The authors declare no competing financial interest.

The mechanisms used in this work as well as code to generate the figures is available in the online data repository Zenodo with DOI: 10.5281/zenodo.4275169.

■ ACKNOWLEDGMENTS

Funding was provided by the National Science Foundation under award number CHE-1709993. M.J.G. was supported by a National Science Foundation Graduate Research Fellowship under Grant No. 1122374.

■ REFERENCES

(1) Ahmed, M.; Pickova, J.; Ahmad, T.; Liaquat, M.; Farid, A.; Jahangir, M. Oxidation of Lipids in Foods. *Sarhad J. Agric.* **2016**, *32*, 230−238.

(2) Birol, F. *Key World Energy Statistics 2017*; International Energy Agency (IEA), 2017.

(3) Heald, C. L.; Kroll, J. H. The Fuel of Atmospheric Chemistry: Toward a Complete Description of Reactive Organic Carbon. *Sci. Adv.* **2020**, *6*, No. eaay8967.

(4) Wang, Z.; Herbinet, O.; Hansen, N.; Battin-Leclerc, F. Exploring Hydroperoxides in Combustion: History, Recent Advances and Perspectives. *Prog. Energy Combust. Sci.* **2019**, *73*, 132−181.

(5) Zhao, P.; Liang, W.; Deng, S.; Law, C. K. Initiation and Propagation of Laminar Premixed Cool Flames. *Fuel* **2016**, *166*, 477−487.

(6) Orlando, J. J.; Tyndall, G. S. Laboratory Studies of Organic Peroxy Radical Chemistry: An Overview with Emphasis on Recent Issues of Atmospheric Significance. *Chem. Soc. Rev.* **2012**, *41*, 6294−6317.

(7) Ingold, K. U. Peroxy Radicals. *Acc. Chem. Res.* **1969**, *2*, 1−9.

(8) Berndt, T.; Scholz, W.; Mentler, B.; Fischer, L.; Herrmann, H.; Kulmala, M.; Hansel, A. Accretion Product Formation from Self- and Cross-Reactions of RO_2 Radicals in the Atmosphere. *Angew. Chem., Int. Ed.* **2018**, *57*, 3820−3824.

(9) Nozière, B.; Fache, F. Reactions of Organic Peroxy Radicals, RO_2, with Substituted and Biogenic Alkenes at Room Temperature: Unsuspected Sinks for Some RO_2 in the Atmosphere. *Chem. Sci.* **2021**, *12*, 11676−11683.

(10) Johnson, D.; Price, D. W.; Marston, G. Correlation-Type Structure Activity Relationships for the Kinetics of Gas-Phase RO_2 Self-Reactions and Reaction with HO_2. *Atmos. Environ.* **2004**, *38*, 1447−1458.

(11) Fittschen, C.; Al Ajami, M.; Batut, S.; Ferracci, V.; Archer-Nicholls, S.; Archibald, A. T.; Schoemaecker, C. ROOOH: The Missing Piece of the Puzzle for OH Measurements in Low NO Environments. *Atmos. Chem. Phys.* **2019**, *19*, 349−362.

(12) Stark, M. S. Epoxidation of Alkenes by Peroxyl Radicals in the Gas Phase: Structure-Activity Relationships. *J. Phys. Chem. A* **1997**, *101*, 8296−8301.
(13) Vereecken, L.; Nozière, B. H Migration in Peroxy Radicals under Atmospheric Conditions. *Atmos. Chem. Phys.* **2020**, *20*, 7429−7458.
(14) Novelli, A.; Vereecken, L.; Bohn, B.; Dorn, H.-P.; Gkatzelis, G. I.; Hofzumahaus, A.; Holland, F.; Reimer, D.; Rohrer, F.; Rosanka, S.; et al. Importance of Isomerization Reactions for OH Radical Regeneration from the Photo-Oxidation of Isoprene Investigated in the Atmospheric Simulation Chamber SAPHIR. *Atmos. Chem. Phys.* **2020**, *20*, 3333−3355.
(15) Hyttinen, N.; Knap, H. C.; Rissanen, M. P.; Jørgensen, S.; Kjaergaard, H. G.; Kurtén, T. Unimolecular HO_2 Loss from Peroxy Radicals Formed in Autoxidation Is Unlikely under Atmospheric Conditions. *J. Phys. Chem. A* **2016**, *120*, 3588−3595.
(16) Vereecken, L.; Müller, J.-F.; Peeters, J. Low-Volatility Poly-Oxygenates in the OH-Initiated Atmospheric Oxidation of α-Pinene: Impact of Non-Traditional Peroxyl Radical Chemistry. *Phys. Chem. Chem. Phys.* **2007**, *9*, 5241−5248.
(17) Vereecken, L.; Peeters, J. Nontraditional (Per)Oxy Ring-Closure Paths in the Atmospheric Oxidation of Isoprene and Monoterpenes. *J. Phys. Chem. A* **2004**, *108*, 5197−5204.
(18) Møller, K. H.; Otkjær, R. V.; Chen, J.; Kjaergaard, H. G. Double Bonds Are Key to Fast Unimolecular Reactivity in First-Generation Monoterpene Hydroxy Peroxy Radicals. *J. Phys. Chem. A* **2020**, *124*, 2885−2896.
(19) Vereecken, L.; Vu, G.; Wahner, A.; Kiendler-Scharr, A.; T Nguyen, H. M. A Structure Activity Relationship for Ring Closure Reactions in Unsaturated Alkylperoxy Radicals. *Phys. Chem. Chem. Phys.* **2021**, *23*, 16564−16576.
(20) Yao, Q.; Sun, X.-H.; Li, Z.-R.; Chen, F.-F.; Li, X.-Y. Pressure-Dependent Rate Rules for Intramolecular H-Migration Reactions of Hydroperoxyalkylperoxy Radicals in Low Temperature. *J. Phys. Chem. A* **2017**, *121*, 3001−3018.
(21) Wijaya, C. D.; Sumathi, R.; Green, W. H. Thermodynamic Properties and Kinetic Parameters for Cyclic Ether Formation from Hydroperoxyalkyl Radicals. *J. Phys. Chem. A* **2003**, *107*, 4908−4920.
(22) Villano, S. M.; Huynh, L. K.; Carstensen, H. H.; Dean, A. M. High-Pressure Rate Rules for Alkyl + O_2 Reactions. 2. the Isomerization, Cyclic Ether Formation, and β-Scission Reactions of Hydroperoxy Alkyl Radicals. *J. Phys. Chem. A* **2012**, *116*, 5068−5089.
(23) Cheng, C. T.; Chan, M. N.; Wilson, K. R. Importance of Unimolecular HO_2 Elimination in the Heterogeneous OH Reaction of Highly Oxygenated Tartaric Acid Aerosol. *J. Phys. Chem. A* **2016**, *120*, 5887−5896.
(24) Welz, O.; Klippenstein, S. J.; Harding, L. B.; Taatjes, C. A.; Zádor, J. Unconventional Peroxy Chemistry in Alcohol Oxidation: The Water Elimination Pathway. *J. Phys. Chem. Lett.* **2013**, *4*, 350−354.
(25) Ray, D. J. M.; Redfearn, A.; Waddington, D. J. Gas-Phase Oxidation of Alkenes: Decomposition of Hydroxy-Substituted Peroxyl Radicals. *J. Chem. Soc., Perkin Trans. 2* **1973**, *0*, 540−543.
(26) Jørgensen, S.; Knap, H. C.; Otkjær, R. V.; Jensen, A. M.; Kjeldsen, M. L. H.; Wennberg, P. O.; Kjaergaard, H. G. Rapid Hydrogen Shift Scrambling in Hydroperoxy-Substituted Organic Peroxy Radicals. *J. Phys. Chem. A* **2016**, *120*, 266−275.
(27) Goldsmith, C. F.; Green, W. H.; Klippenstein, S. J. Role of O_2 + QOOH in Low-Temperature Ignition of Propane. 1. Temperature and Pressure Dependent Rate Coefficients. *J. Phys. Chem. A* **2012**, *116*, 3325−3346.
(28) Liu, Z.; Nguyen, V. S.; Harvey, J.; Müller, J.-F.; Peeters, J. Theoretically Derived Mechanisms of HPALD Photolysis in Isoprene Oxidation. *Phys. Chem. Chem. Phys.* **2017**, *19*, 9096−9106.
(29) Crounse, J. D.; Nielsen, L. B.; Jørgensen, S.; Kjaergaard, H. G.; Wennberg, P. O. Autoxidation of Organic Compounds in the Atmosphere. *J. Phys. Chem. Lett.* **2013**, *4*, 3513−3520.
(30) Merchant, S. S.; Goldsmith, C. F.; Vandeputte, A. G.; Burke, M. P.; Klippenstein, S.; Green, W. H. Understanding Low-Temperature First Stage Ignition Delay: Propane. *Combust. Flame* **2015**, *162*, 3658−3673.
(31) Carter, W. P. L.; Darnall, K. R.; Lloyd, A. C.; Winer, A. M.; Pitts, J. N. Evidence for Alkoxy Radical Isomerization in Photooxidations of C4-C6 Alkanes under Simulated Atmospheric Conditions. *Chem. Phys. Lett.* **1976**, *42*, 22−27.
(32) Crounse, J. D.; Paulot, F.; Kjaergaard, H. G.; Wennberg, P. O. Peroxy Radical Isomerization in the Oxidation of Isoprene. *Phys. Chem. Chem. Phys.* **2011**, *13*, 13607−13613.
(33) Crounse, J. D.; Knap, H. C.; Ørnsø, K. B.; Jørgensen, S.; Paulot, F.; Kjaergaard, H. G.; Wennberg, P. O. Atmospheric Fate of Methacrolein. 1. Peroxy Radical Isomerization Following Addition of OH and O_2. *J. Phys. Chem. A* **2012**, *116*, 5756−5762.
(34) Glaude, P. A.; Marinov, N.; Koshiishi, Y.; Matsunaga, N.; Hori, M. Kinetic Modeling of the Mutual Oxidation of NO and Larger Alkanes at Low Temperature. *Energy Fuels* **2005**, *19*, 1839−1849.
(35) Alzueta, M. U.; Muro, J.; Bilbao, R.; Glarborg, P. Oxidation of Dimethyl Ether and Its Interaction with Nitrogen Oxides. *Isr. J. Chem.* **1999**, *39*, 73−86.
(36) Anderlohr, J.; Bounaceur, R.; Piresdacruz, A.; Battinleclerc, F. Modeling of Autoignition and NO Sensitization for the Oxidation of IC Engine Surrogate Fuels. *Combust. Flame* **2009**, *156*, 505−521.
(37) Andrae, J. C. G. Kinetic Modeling of the Influence of NO on the Combustion Phasing of Gasoline Surrogate Fuels in an HCCI Engine. *Energy Fuels* **2013**, *27*, 7098−7107.
(38) Heiss, A.; Sahetchian, K. Isomerization Reactions of the n-C_4H_9O and n-OOC_4H_8OH Radicals in Oxygen. *Int. J. Chem. Kinet.* **1996**, *28*, 531−544.
(39) Sehested, J.; Møgelberg, T.; Wallington, T. J.; Kaiser, E. W.; Nielsen, O. J. Dimethyl Ether Oxidation: Kinetics and Mechanism of the CH_3OCH_2 + O_2 Reaction at 296 K and 0.38-940 Torr Total Pressure. *J. Phys. Chem. A* **1996**, *100*, 17218−17225.
(40) Orlando, J. J. The Atmospheric Oxidation of Diethyl Ether: Chemistry of the C_2H_5−O−$CH(O\cdot)CH_3$ Radical between 218 and 335 K. *Phys. Chem. Chem. Phys.* **2007**, *9*, 4189−4199.
(41) Peeters, J.; Nguyen, T. L.; Vereecken, L. HO_x Radical Regeneration in the Oxidation of Isoprene. *Phys. Chem. Chem. Phys.* **2009**, *11*, 5935−5939.
(42) da Silva, G.; Graham, C.; Wang, Z.-F. Unimolecular β-Hydroxyperoxy Radical Decomposition with OH Recycling in the Photochemical Oxidation of Isoprene. *Environ. Sci. Technol.* **2010**, *44*, 250−256.
(43) Ehn, M.; a Thornton, J.; Kleist, E.; Sipilä, M.; Junninen, H.; Pullinen, I.; Springer, M.; Rubach, F.; Tillmann, R.; Lee, B.; et al. A Large Source of Low-Volatility Secondary Organic Aerosol. *Nature* **2014**, *506*, 476−479.
(44) Bianchi, F.; Kurtén, T.; Riva, M.; Mohr, C.; Rissanen, M. P.; Roldin, P.; Berndt, T.; Crounse, J. D.; Wennberg, P. O.; Mentel, T. F.; et al. Highly Oxygenated Organic Molecules (HOM) from Gas-Phase Autoxidation Involving Peroxy Radicals: A Key Contributor to Atmospheric Aerosol. *Chem. Rev.* **2019**, *119*, 3472−3509.
(45) Praske, E.; Otkjær, R. V.; Crounse, J. D.; Hethcox, J. C.; Stoltz, B. M.; Kjaergaard, H. G.; Wennberg, P. O. Atmospheric Autoxidation Is Increasingly Important in Urban and Suburban North America. *Proc. Natl. Acad. Sci. U.S.A.* **2018**, *115*, 64−69.
(46) Møller, K. H.; Otkjær, R. V.; Hyttinen, N.; Kurtén, T.; Kjaergaard, H. G. Cost-Effective Implementation of Multiconformer Transition State Theory for Peroxy Radical Hydrogen Shift Reactions. *J. Phys. Chem. A* **2016**, *120*, 10072−10087.
(47) Anglada, J. M.; Martins-Costa, M.; Francisco, J. S.; Ruiz-López, M. F. Interconnection of Reactive Oxygen Species Chemistry across the Interfaces of Atmospheric, Environmental, and Biological Processes. *Acc. Chem. Res.* **2015**, *48*, 575−583.
(48) Wang, Z.; Popolan-Vaida, D. M.; Chen, B.; Moshammer, K.; Mohamed, S. Y.; Wang, H.; Sioud, S.; Raji, M. A.; Kohse-Höinghaus, K.; Hansen, N.; et al. Unraveling the Structure and Chemical Mechanisms of Highly Oxygenated Intermediates in Oxidation of Organic Compounds. *Proc. Natl. Acad. Sci. U.S.A.* **2017**, *114*, 13102−13107.
(49) Wang, Z.; Ehn, M.; Rissanen, M. P.; Garmash, O.; Quéléver, L.; Xing, L.; Monge-Palacios, M.; Rantala, P.; Donahue, N. M.; Berndt, T.;

et al. Efficient Alkane Oxidation under Combustion Engine and Atmospheric Conditions. *Commun. Chem.* **2021**, *4*, No. 18.
(50) Otkjær, R. V.; Jakobsen, H. H.; Tram, C. M.; Kjaergaard, H. G. Calculated Hydrogen Shift Rate Constants in Substituted Alkyl Peroxy Radicals. *J. Phys. Chem. A* **2018**, *122*, 8665−8673.
(51) Villano, S. M.; Huynh, L. K.; Carstensen, H. H.; Dean, A. M. High-Pressure Rate Rules for Alkyl + O_2 Reactions. 1. the Dissociation, Concerted Elimination, and Isomerization Channels of the Alkyl Peroxy Radical. *J. Phys. Chem. A* **2011**, *115*, 13425−13442.
(52) Møller, K. H.; Kurtén, T.; Bates, K. H.; Thornton, J. A.; Kjaergaard, H. G. Thermalized Epoxide Formation in the Atmosphere. *J. Phys. Chem. A* **2019**, *123*, 10620−10630.
(53) Jenkin, M. E.; Valorso, R.; Aumont, B.; Rickard, A. R. Estimation of Rate Coefficients and Branching Ratios for Reactions of Organic Peroxy Radicals for Use in Automated Mechanism Construction. *Atmos. Chem. Phys.* **2019**, *19*, 7691−7717.
(54) Goldman, M. J.; Yee, N. W.; Kroll, J. H.; Green, W. H. Pressure-Dependent Kinetics of Peroxy Radicals Formed in Isobutanol Combustion. *Phys. Chem. Chem. Phys.* **2020**, *22*, 19802−19815.
(55) Liu, M.; Grinberg Dana, A.; Johnson, M. S.; Goldman, M. J.; Jocher, A.; Payne, A. M.; Grambow, C. A.; Han, K.; Yee, N. W.; Mazeau, E. J.; et al. Reaction Mechanism Generator v3.0: Advances in Automatic Mechanism Generation. *J. Chem. Inf. Model.* **2021**, *61*, 2686−2696.
(56) Curran, H. J. *AramcoMech*; NUI: Galway, 2017.
(57) Gallagher, S. M.; Curran, H. J.; Metcalfe, W. K.; Healy, D.; Simmie, J. M.; Bourque, G. A Rapid Compression Machine Study of the Oxidation of Propane in the Negative Temperature Coefficient Regime. *Combust. Flame* **2008**, *153*, 316−333.
(58) Atkinson, R. Gas-Phase Tropospheric Chemistry of Volatile Organic Compounds: 1. Alkanes and Alkenes. *J. Phys. Chem. Ref. Data* **1997**, *26*, 215−290.
(59) Allen, J. W.; Goldsmith, C. F.; Green, W. H. Automatic Estimation of Pressure-Dependent Rate Coefficients. *Phys. Chem. Chem. Phys.* **2012**, *14*, 1131−1155.
(60) Gao, C. W.; Allen, J. W.; Green, W. H.; West, R. H. Reaction Mechanism Generator: Automatic Construction of Chemical Kinetic Mechanisms. *Comput. Phys. Commun.* **2016**, *203*, 212−225.
(61) Miyoshi, A. Systematic Computational Study on the Unimolecular Reactions of Alkylperoxy (RO_2), Hydroperoxyalkyl (QOOH), and Hydroperoxyalkylperoxy (O_2QOOH) Radicals. *J. Phys. Chem. A* **2011**, *115*, 3301−3325.
(62) da Silva, G.; Bozzelli, J. W.; Liang, L.; Farrell, J. T. Ethanol Oxidation: Kinetics of the α-Hydroxyethyl Radical. O_2 Reaction. *J. Phys. Chem. A* **2009**, *113*, 8923−8933.
(63) Sarathy, S. M.; Vranckx, S.; Yasunaga, K.; Mehl, M.; Oßwald, P.; Metcalfe, W. K.; Westbrook, C. K.; Pitz, W. J.; Kohse-Höinghaus, K.; Fernandes, R. X.; et al. A Comprehensive Chemical Kinetic Combustion Model for the Four Butanol Isomers. *Combust. Flame* **2012**, *159*, 2028−2055.
(64) Goodwin, D. G.; Moffat, H. K.; Speth, R. L. Cantera: An Object-Oriented Software Toolkit for Chemical Kinetics, Thermodynamics, and Transport Processes, 2016. http://cantera.org.
(65) Bugler, J.; Somers, K. P.; Silke, E. J.; Curran, H. J. Revisiting the Kinetics and Thermodynamics of the Low-Temperature Oxidation Pathways of Alkanes: A Case Study of the Three Pentane Isomers. *J. Phys. Chem. A* **2015**, *119*, 7510−7527.
(66) Welz, O.; Savee, J. D.; Eskola, A. J.; Sheps, L.; Osborn, D. L.; Taatjes, C. A. Low-Temperature Combustion Chemistry of Biofuels: Pathways in the Low-Temperature (550−700K) Oxidation Chemistry of Isobutanol and Tert-Butanol. *Proc. Combust. Inst.* **2013**, *34*, 493−500.
(67) Barber, V. P.; Green, W. H.; Kroll, J. H. Screening for New Pathways in Atmospheric Oxidation Chemistry with Automated Mechanism Generation. *J. Phys. Chem. A* **2021**, *125*, 6772−6788.
(68) Zhao, H.; Wu, L.; Patrick, C.; Zhang, Z.; Rezgui, Y.; Yang, X.; Wysocki, G.; Ju, Y. Studies of Low Temperature Oxidation of n-Pentane with Nitric Oxide Addition in a Jet Stirred Reactor. *Combust. Flame* **2018**, *197*, 78−87.
(69) Zhao, H.; Dana, A. G.; Zhang, Z.; Green, W. H.; Ju, Y. Experimental and Modeling Study of the Mutual Oxidation of n-Pentane and Nitrogen Dioxide at Low and High Temperatures in a Jet Stirred Reactor. *Energy* **2018**, *165*, 727−738.
(70) Hebbar, G. S. NO_x from Diesel Engine Emission and Control Strategies: A Review. *Int. J. Mech. Eng. Rob. Res.* **2014**, *3*, No. 471.
(71) Bates, K. H.; Jacob, D. J. A New Model Mechanism for Atmospheric Oxidation of Isoprene: Global Effects on Oxidants, Nitrogen Oxides, Organic Products, and Secondary Organic Aerosol. *Atmos. Chem. Phys.* **2019**, *19*, 9613−9640.

https://doi.org/10.1021/acs.jpca.1c07203
J. Phys. Chem. A 2021, 125, 10303−10314